

# Characterizing PCB Rogowski Coil Bandwidth with Vector Network Analyzer

Chi-Yuan Huang

Dept. of Electrical Engineering  
National Taiwan University  
Taipei, Taiwan  
f11921029@ntu.edu.tw

Sohaib Qazi

PE group, Faculty EEMCS  
University of Twente  
Enschede, The Netherlands  
sohaib.qazi@utwente.nl

Yaow-Ming Chen

Dept. of Electrical Engineering  
National Taiwan University  
Taipei, Taiwan  
ntuymchen@ntu.edu.tw

Thiago Batista Soeiro

PE group, Faculty EEMCS  
University of Twente  
Enschede, The Netherlands  
t.batistasoeiro@utwente.nl

**Abstract**—This paper presents a fast modeling method for characterizing the bandwidth of a PCB Rogowski coil using a Vector Network Analyzer (VNA). By measuring the reflection coefficient of the Rogowski coil with VNA, the stray inductance and capacitance can be extracted to model the coil's frequency response. This approach overcomes the frequency limitations of impedance analyzers and the heavy computational effort required by electromagnetic simulation software. Experimental validation demonstrates a correlation between the calculated lumped model and the measured frequency response, which confirms the method's accuracy. The proposed method provides a fast and reliable way to determine the Rogowski coil's bandwidth, aiding in its application for isolated high-frequency current sensing.

**Index Terms**—Rogowski Coil, Bandwidth, Vector Network Analyzer.

## I. INTRODUCTION

Rogowski coils are widely used where a contactless current measurement is needed due to the high voltage or large current [1]–[3]. These air-core, flexible coils can encircle the conductor without interrupting the circuit and can be shaped to meet various geometric requirements. The Rogowski coil operates based on Faraday's law [4], it detects the rate of change of current,  $di(t)/dt$ , and an integrator is used to convert the induced voltage into a signal  $i'(t)$ , which is proportional to the actual current  $i(t)$ .

The structure of a PCB Rogowski coil is shown in Fig. 1 and its lumped model is shown in Fig. 2, where  $M$  is the mutual inductance of the Rogowski coil,  $R_c$  is the resistance of the PCB trace,  $L_c$  is the inductance of the PCB trace,  $C_c$  is the stray capacitance between the coil's two terminals, and  $R_d$  is the damping resistor. To characterize the bandwidth of the coil, it is necessary to know the  $R_c$ ,  $L_c$ , and  $C_c$  in order to select the appropriate  $R_d$ , as the selection of  $R_d$  is the trade-off between fast response and signal integrity that could suffer from circuit resonances [5], [6].

Measuring the  $L_c$  and  $C_c$  can be challenging as  $L_c$  can fall in the nH range and  $C_c$  in the pF range for the high bandwidth (over 100 MHz) Rogowski coil [7], which may be challenging to measure due to the limited frequency range of the impedance analyzer. Although it is possible to extract  $L_c$  and  $C_c$  using electromagnetic simulation software such as Ansys HFSS or COMSOL Multiphysics [8], [9]. However,

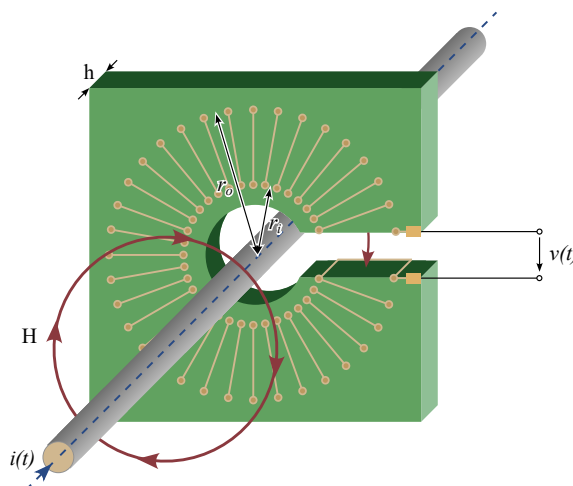


Fig. 1. The structure of PCB Rogowski coil.

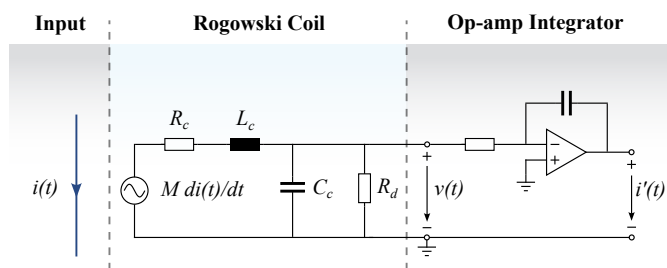


Fig. 2. Simplified PCB Rogowski coil's lumped circuit model with integrator.

accurate modeling requires significant computational effort. Also, variation in environment factors such as temperature and humidity will affect the effective value of the dielectric constant, these PCB fabrication imperfections are nearly impossible to model.

This paper presents a fast method for characterizing a PCB Rogowski coil by extracting its stray components using a Vector Network Analyzer (VNA). The extracted values are then used to construct a lumped model of the Rogowski coil and determine its bandwidth.

## II. STRAY COMPONENTS MEASUREMENT

A VNA is commonly used to characterize RF devices by measuring the scattering parameters (S-parameters) of the device under test (DUT). Depending on the impedance of the DUT, different measurement methods are preferred: one-port reflection method, shunt-through (two-port shunt) method, and series-through (two-port series) method [10]. The shunt-through method is suitable for low-impedance DUTs ( $Z_X \ll 50 \Omega$ ), the series-through method is suitable for high-impedance DUTs ( $Z_X \gg 50 \Omega$ ), while the one-port reflection method is suitable for DUTs with impedance close to  $50 \Omega$  [11], [12]. Fig. 3 illustrates the measurement setup for determining the DUT's impedance  $Z_X$  using these three methods. The one-port reflection method is chosen in this work for simplicity, as two-port measurements require a dedicated fixture to perform proper calibration.

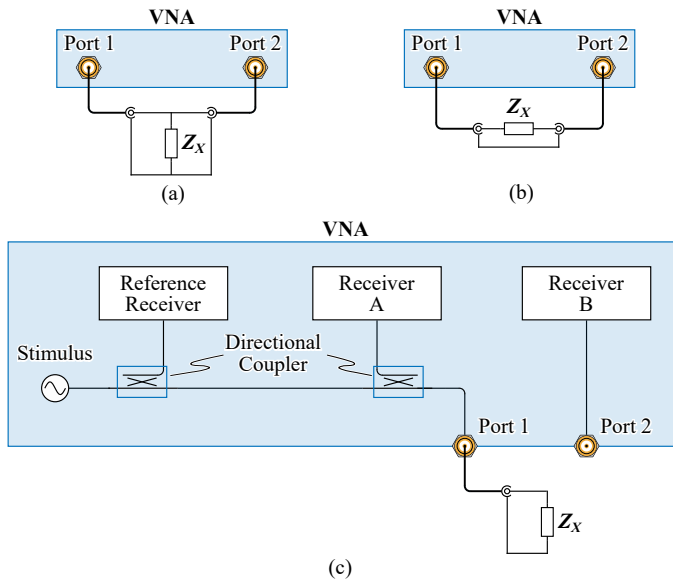


Fig. 3. Impedance measurement setup of VNA-based approach. (a) Shunt-through method. (b) Series-through method. (c) One-port reflection method.

### A. One-port Reflection Method

A VNA in a one-port configuration measures the magnitude and phase of the DUT's reflection coefficient  $\Gamma$ , or  $S_{11}$ . Fig. 3(c) illustrates a simplified VNA structure with the one-port reflection measurement setup. The key components of the VNA include RF stimulus, directional coupler, and RF receiver.

In Fig. 3(c), the RF stimulus first generates an incident signal, which is then first detected by the reference receiver via a directional coupler and travels to the DUT from port 1. After the incident signal hits DUT, the reflected signal travels back to port 1 and is then detected by receiver A via the directional coupler. The reflection coefficient,  $\Gamma$ , is defined as the ratio between the vector voltage  $V_R$  detected by the reference receiver and the reflected signal  $V_A$  detected by receiver A, as expressed in (1), where the impedance

of DUT  $Z_X$  can then be calculated from  $\Gamma$  using (2). The relation between DUT's impedance  $Z_X$ , system characteristic impedance  $Z_0$ , and  $\Gamma$  is shown in Fig. 4.

$$\Gamma = \frac{V_A}{V_R} = S_{11} \quad (1)$$

$$Z_X = Z_0 \cdot \frac{1 + \Gamma}{1 - \Gamma} = Z_0 \cdot \frac{1 + S_{11}}{1 - S_{11}} \quad (2)$$

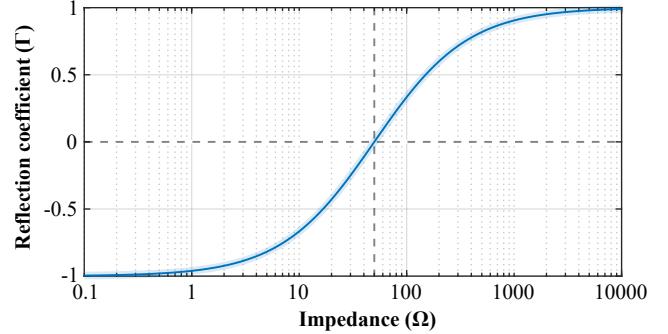


Fig. 4. The relationship between  $\Gamma$  and impedance of  $Z_x$  when  $Z_0$  equals to  $50 \Omega$  in one-port reflection method.

Considering the measurement setup in Fig. 3(c), when  $Z_X$  is close to  $Z_0$  ( $Z_0 = 50 \Omega$  in most of the VNAs), the one-port reflection method yields the highest sensitivity because the directional coupler inside VNA detects null, and  $\Gamma$  significantly changes with a slight change in the impedance. It should be mentioned that the measurement sensitivity of the one-port reflection method decreases, since the gradient of  $\Gamma$  will converge to 0 for the lower and higher impedance, as shown in Fig. 4. Thus, to get the most accurate measurement result, the impedance of the  $L_c$  and  $C_c$  of the Rogowski coil should be measured at the frequency when  $Z_X = Z_0$ , to ensure the gradient of  $\Gamma$  is maximum.

### B. Lumped Model Extraction

Fig. 5 shows the stray components measurement setup for the PCB Rogowski coil under test using the one-port reflection method. The stray components are measured with a LibreVNA, an open-source 2-port VNA with the frequency range from 100 kHz to 6 GHz, and a dynamic range greater than 90 dB below 3 GHz.

To accurately measure the stray components of the Rogowski coil, short-open-load-through (SOLT) calibration and de-embedding are necessary for the VNA. After the calibration, the reference plane of the impedance measurement should be on the connection between the SMA connector and the PCB. This SOLT calibration and de-embedding eliminate the systematic error caused by the reference receiver, receiver A, and the SMA connector. The detailed calibration method is beyond the scope of this paper and will not be discussed here.

Fig. 6 shows the  $S_{11}$  of the PCB Rogowski coil in the Smith Chart from 1 MHz to 1 GHz, measured by the one-port reflection setup shown in Fig. 3(c). In Fig. 6, the  $S_{11}$

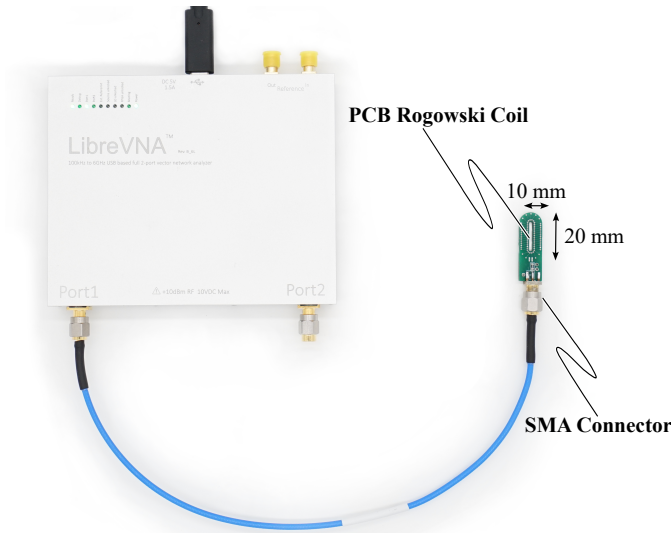


Fig. 5. Stray components measurement setup for PCB Rogowski under test using one-port reflection method.

trace begins near the “Short” location, where the impedance of  $Z_X$  is dominated by  $R_c$ , which is close to a short circuit at lower frequencies. As the frequency increases, the  $Z_X$  moves toward the upper part of the Smith chart, indicating that  $Z_X$  is dominated by  $L_c$  and thus behaves inductively. As the frequency continues to increase,  $Z_X$  approaches the “Open” location, as  $L_c$  and  $C_c$  form a parallel  $L_c$  resonant tank, causing  $Z_X$  to reach its maximum impedance at resonance. Nevertheless, as the frequency increases further,  $Z_X$  moves toward the lower part of the Smith chart, indicating that  $Z_X$  is dominated by  $C_c$  and thus behaves capacitively.

Based on Fig. 6, it can be seen that the measured  $R_c$  is relatively small compared to  $Z_0$  and can be neglected when extracting the values of  $L_c$  and  $C_c$ . By plotting constant reactance arcs of  $50 \Omega$  (both inductive and capacitive) on the Smith chart,  $L_c$  and  $C_c$  can be determined by identifying the intersections with the constant reactance arcs. This approach assumes the Rogowski coil behaves as a pure inductor or capacitor (i.e.,  $R_c$  is negligible) with an impedance equal to  $50 \Omega$ . From the intersections with the constant reactance arcs, the inductance of  $L_c$  is measured to be 286 nH at 27.7 MHz, while the capacitance of  $C_c$  is 3.27 pF at 972.7 MHz, and the characteristic impedance of the coil  $Z_c$ , can then be determined using (3).

$$Z_c = \sqrt{\frac{L_c}{C_c}} \quad (3)$$

To measure the resistance of the PCB trace  $R_c$ , the shunt-through method shown in Fig. 3(a) or the 4-wire (Kelvin sense) resistance measurement technique using a multimeter can be achieved.

Next, the mutual inductance between the current conductor and Rogowski coil,  $M$ , can be determined by Faraday’s Law.

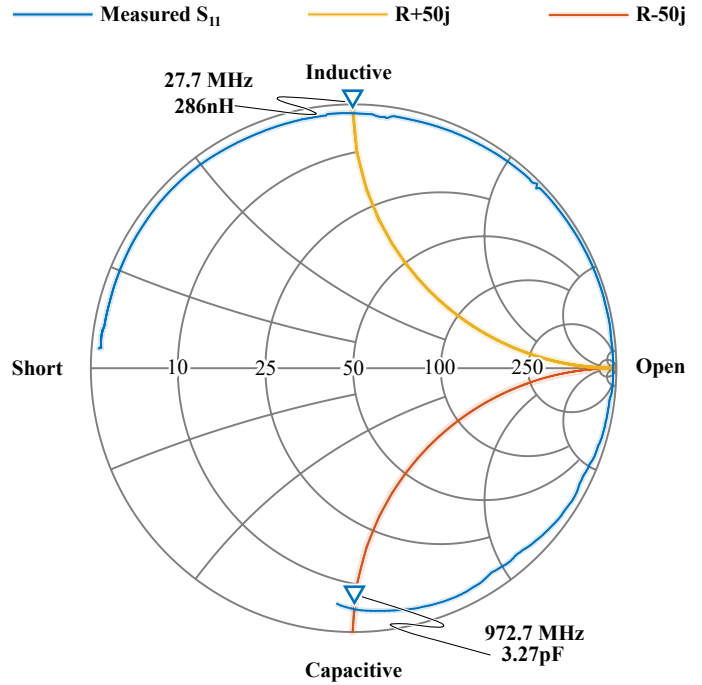


Fig. 6. Measured  $S_{11}$  of PCB Rogowski coil under test from 1 MHz to 1 GHz. From the intersections with the constant reactance arcs of  $50 \Omega$ , the  $L_c$  and  $C_c$  can be obtained, yielding  $Z_c \approx 300 \Omega$ .

From Fig. 1, the instantaneous voltage  $v(t)$  induced by a time-varying magnetic flux  $\phi$  can be expressed by (4), where  $N$  is the total number of turns in the Rogowski coil.

$$v(t) = N \cdot \frac{d\phi(t)}{dt} \quad (4)$$

The magnetic flux through the  $k$ th turn of the Rogowski coil,  $\phi_k$ , is defined by (5), where  $\mu_0$  is the permeability constant equal to  $4\pi \cdot 10^{-7}$  H/m,  $h$  is the thickness of the PCB,  $r_{i,k}$  and  $r_{o,k}$  are the distance from the center of the coil to the inner and outer of the coil at the  $k$ th turn, as shown in Fig. 1.

$$\phi_k = \frac{\mu_0 h}{2\pi} \cdot \ln \frac{r_{o,k}}{r_{i,k}} \quad (5)$$

By summing the flux over all  $N$  turns on the Rogowski coil, mutual inductance  $M$  can be calculated by (6) [13].

$$M = N \cdot \phi_{total} \quad (6)$$

With the  $M$ , along with  $R_c$ ,  $L_c$ , and  $C_c$ , the transfer function of the Rogowski coil’s lumped model in Fig. 2 can be constructed:

$$v(t) = \frac{di(t)}{dt} \cdot \frac{M}{s^2 L_c C_c + S(R_c C_c) + (1 + \frac{L_c}{R_d})} \quad (7)$$

The parameters extracted from the PCB Rogowski coil under test in Fig. 5 are listed in Table I. To achieve the proper signal termination for the Rogowski coil, the damping resistor is chosen to be  $R_d = Z_c \approx 300 \Omega$ .

TABLE I  
EXTRACTED PCB ROGOWSKI COIL PARAMETERS

Description	Parameter	Value
Number of Turns	$N$	20
Height of PCB	$h$	1.6 mm
Mutual Inductance	$M$	4.27 nF
Equivalent Resistance	$R_c$	0.89 $\Omega$
Equivalent Inductance	$L_c$	287 nH
Equivalent Capacitance	$C_c$	3.27 pF

### III. EXPERIMENTAL EVALUATION

To evaluate the accuracy of the proposed fast characterization method, a frequency domain comparison is performed between the measured frequency results and the analytical lumped model in (7), using the component values listed in Table I.

In addition to the frequency domain comparison, a step response comparison with the current shunt resistor is also performed to provide a more practical assessment of the Rogowski coil's performance.

#### A. Frequency Response Measurement

Fig. 7 illustrates the frequency response measurement setup for the Rogowski coil. To capture a wide frequency range of frequency response, two complementary instruments were used together to compensate for the frequency limitations of each instrument: the 350 MHz MXO58 oscilloscope from Rohde & Schwarz, operated in its built-in frequency response analyzer (FRA) function, and a LibreVNA, configured to measure the  $S_{21}$  response.

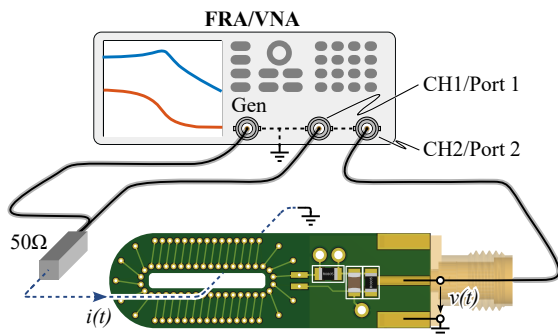


Fig. 7. Measurement setup of the Rogowski coil response.

In Fig. 7, the signal generator (or stimulus in VNA) with 50  $\Omega$  output impedance is connected to a 50  $\Omega$  load resistor. The Rogowski coil then senses the current passing through the load resistor, and the FRA/VNA then performs frequency response analysis/ $S_{21}$  measurement by comparing the stimulus from the generator with the voltage induced at the coil's output. The equivalent circuit of the frequency response analysis setup is illustrated in Fig. 8.

It is important to ensure that the load resistor matches the system impedance (50  $\Omega$  in this experimental setup) to avoid signal reflection caused by impedance mismatch, as any reflection energy will distort the measured frequency response.

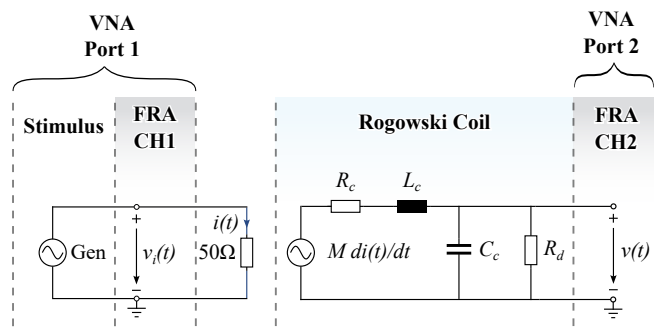


Fig. 8. The equivalent circuit of the frequency response measurement setup.

Since the Rogowski coil under test has  $R_d = 300 \Omega$ , the 50  $\Omega$  input impedance of the oscilloscope and VNA will make the Rogowski coil overdamped. Instead, a transmission line probe with an input resistance of 1 k $\Omega$  is used to probe the output of the Rogowski coil under test.

Fig. 9(a) presents the frequency response comparison between the calculated model and the measurement results. Both the calculated and measured responses in Fig. 9(a) exhibit a 20 dB/dec increase in magnitude, as the frequency increases close to the coil's resonant frequency, the magnitude starts to decline.

The bandwidth of the coil can be determined by identifying the cutoff frequency after adding an ideal integrator, as shown in Fig. 9(b). The calculated model has a bandwidth of 163 MHz, whereas the measured coil has a bandwidth of 143 MHz. This bandwidth deviation occurs because the transmission line probe's impedance is not included in the calculated model. Based on the one-port reflection method shown in Fig. 3, the parasitic capacitance of the transmission line probe of 0.9 pF is measured, which aligns with the calculated bandwidth of the lumped model. It can be further observed from Fig. 9(b) that the sensitivity of the coil deviates from the calculated model. However, the measured sensitivity deviations are below 1 dB across the measured frequency range and can be corrected by external gain adjustment.

#### B. Step Response Measurement

A time domain comparison was conducted between the PCB Rogowski coil under test and the 1 GHz bandwidth 0.1  $\Omega$  current shunt resistor SDN-414-10 from T&M Research Products, which serves as the reference sensor.

In the time domain comparison setup, the output of the generator in Fig. 9 is configured to be a square wave with a 9 ns rise time, while the 0.1  $\Omega$  current shunt resistor is inserted between the generator and the 50  $\Omega$  load resistor. To avoid the bandwidth limitation of the op-amp based integrators, the output of the Rogowski coil under test is integrated with the oscilloscope's math function. Additionally, integration gains were adjusted to compensate for the difference in sensitivity between the two current sensors.

A 400 MHz oscilloscope WaveSurfer 44MXs-B from Teledyne LeCroy is used to capture the time domain comparison

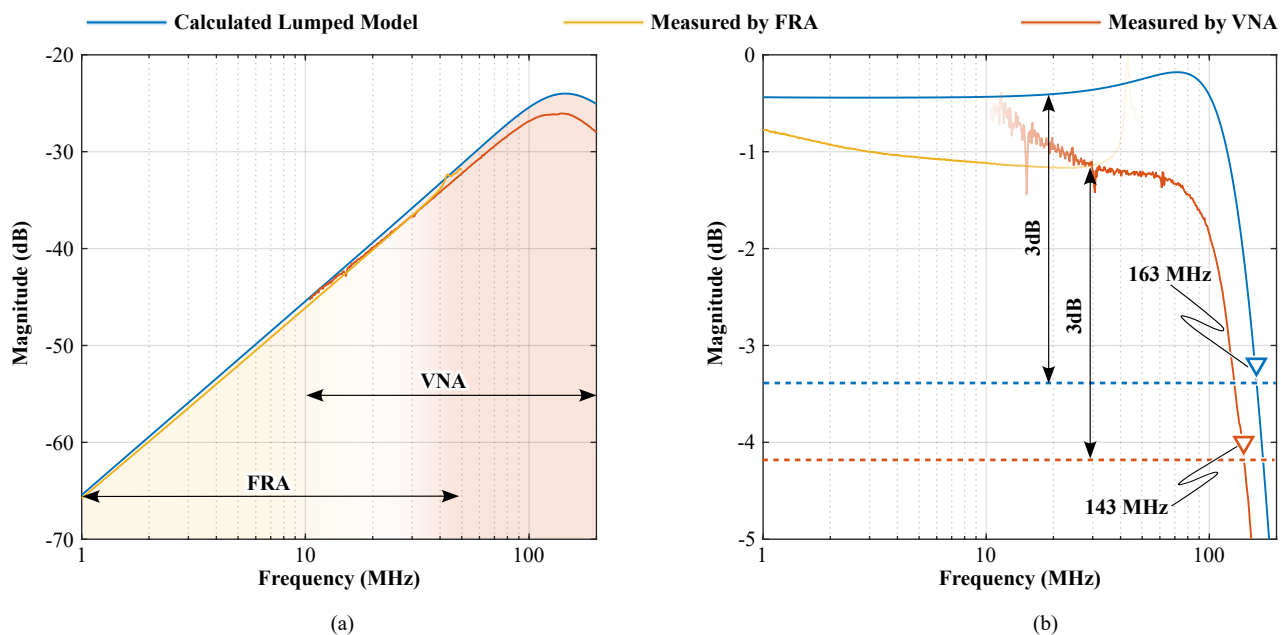


Fig. 9. (a) Comparison of the frequency response between the extracted lumped model and measurement results of the Rogowski coil and (b) frequency response after applying an ideal integrator. The frequency response difference is caused by the influence of the probe's parasitic impedance.

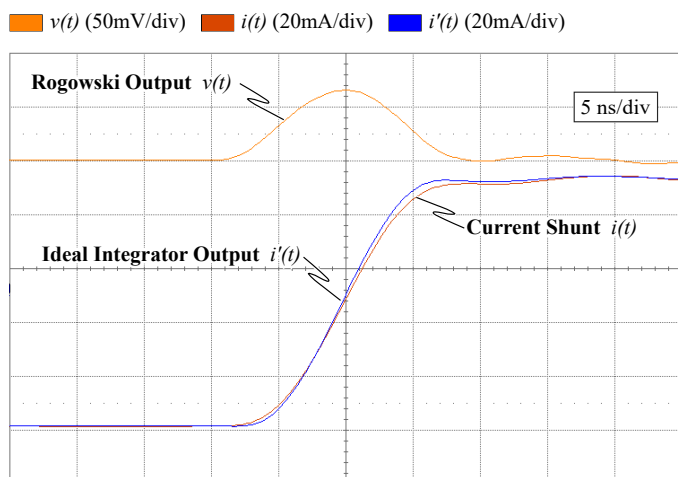


Fig. 10. Comparison of step response between PCB Rogowski under test and SDN-414-10 current shunt resistor.

with the sample rate of 5 GS/s. Fig. 10 shows the key waveforms of the comparison between the PCB Rogowski under test and the current shunt resistor. It can be seen from the top of Fig. 10, the derivation of current step  $di/dt$  from the generator has been captured by the PCB Rogowski coil under test, since the impedance of the generator matches the load resistor, there's no signal reflection observed on the output of either sensor. The bottom of Fig. 10 shows the output of the current shunt resistor and the integrated signal from the PCB Rogowski coil under test using the oscilloscope's math function, which integrates the  $di/dt$  signal back into the step current. The required bandwidth of the sensor to capture a signal with the rise time  $t_r$  can be estimated as

$BW = 0.35/t_r$  [14]. To capture the 9 ns rise time edge, the minimum bandwidth will be 38.8 MHz. Since the PCB Rogowski coil under test has a bandwidth of 143 MHz, the 9 ns rise time current step can be captured by the Rogowski coil and reconstructed by the integrator.

#### IV. CONCLUSION

This paper presents a fast modeling approach for characterizing the PCB Rogowski coil's bandwidth using one-port VNA measurement. The working principle of the VNA impedance measurement setup is first discussed and applied to extract the stray inductance and capacitance of the Rogowski coil. This method overcomes the frequency limits of conventional impedance analyzers and the heavy computational effort of electromagnetic simulation software. Experimental validation demonstrated the correlation between the extracted lumped model and the frequency response analyzer. Although the calculated model frequency response doesn't fully match the measurement results due to the influence of probe parasitics, this modeling approach still offers a fast estimation of the Rogowski coil's usable frequency range. Furthermore, a step response comparison between a reference current sensor provides a practical assessment of the Rogowski coil's performance. Overall, the experimental results verify the accuracy and practicality of the proposed bandwidth characterizing approach.

#### V. ACKNOWLEDGMENT

This work was supported by the Taiwan National Science and Technology Council (NSTC) under Grant No. NSTC 113-2622-E-002-034.

## REFERENCES

- [1] D. Bortis, J. Biela, and J. W. Kolar, "Active gate control for current balancing of parallel-connected igt modules in solid-state modulators," *IEEE Transactions on Plasma Science*, vol. 36, no. 5, pp. 2632–2637, 2008.
- [2] K. Hasegawa, S. Takahara, S. Tabata, M. Tsukuda, and I. Omura, "A new output current measurement method with tiny pcb sensors capable of being embedded in an igt module," *IEEE Transactions on Power Electronics*, vol. 32, no. 3, pp. 1707–1712, 2017.
- [3] S. Mocevic, J. Wang, R. Burgos, D. Boroyevich, M. Jaksic, M. Teimor, and B. Peaslee, "Phase current sensor and short-circuit detection based on rogowski coils integrated on gate driver for 1.2 kv sic mosfet half-bridge module," in *2018 IEEE Energy Conversion Congress and Exposition (ECCE)*, 2018, pp. 393–400.
- [4] Y. Shi, Z. Xin, P. C. Loh, and F. Blaabjerg, "A review of traditional helical to recent miniaturized printed circuit board rogowski coils for power-electronic applications," *IEEE Transactions on Power Electronics*, vol. 35, no. 11, pp. 12 207–12 222, 2020.
- [5] P. S. Niklaus, D. Bortis, and J. W. Kolar, "Beyond 50 mhz bandwidth extension of commercial dc-current measurement sensors with ultra-compact pcb-integrated pickup coils," *IEEE Transactions on Industry Applications*, vol. 58, no. 4, pp. 5026–5041, 2022.
- [6] W. Ray and C. Hewson, "High performance rogowski current transducers," in *Conference Record of the 2000 IEEE Industry Applications Conference. Thirty-Fifth IAS Annual Meeting and World Conference on Industrial Applications of Electrical Energy (Cat. No.00CH37129)*, vol. 5, 2000, pp. 3083–3090 vol.5.
- [7] S. B. Sohaid, X. Tian, N. Jia, H. Cui, W. Zhang, F. Wang, and B. Holzinger, "Pcb rogowski coil with dc sensing for double pulse test applications," *IEEE Transactions on Power Electronics*, vol. 39, no. 4, pp. 4494–4502, 2023.
- [8] X. Zhao, R. Phukan, C.-W. Chang, D. Dong, R. Burgos, A. PLAT, and D. Mustapha, "Design of rogowski coil current sensor integrated with busbar and gate driver for 211 kw sic-based three-level t-type inverter," in *2022 IEEE Energy Conversion Congress and Exposition (ECCE)*, 2022, pp. 1–7.
- [9] Z. Yuan, B. Narayanasamy, Z. Wang, Y. Wang, A. I. Emon, M. Hassan, and F. Luo, "A high accuracy characterization method of busbar parasitic capacitance for three-level converters based on vector network analyzer," in *2021 IEEE Applied Power Electronics Conference and Exposition (APEC)*, 2021, pp. 1543–1548.
- [10] H. Jie, Z. Zhao, F. Fei, K. Y. See, R. Simanjorang, and F. Sasongko, "A survey of impedance measurement methods in power electronics," in *2022 IEEE International Instrumentation and Measurement Technology Conference (I2MTC)*, 2022, pp. 1–6.
- [11] K. Technologies, *Impedance Measurement Handbook*. Keysight Technologies, 2020.
- [12] S. M. Sandler, "Extending the usable range of the 2-port shunt through impedance measurement," in *2016 IEEE MTT-S Latin America Microwave Conference (LAMC)*, 2016, pp. 1–3.
- [13] M. Stecca, P. Tiftikidis, T. B. Soeiro, and P. Bauer, "Gate driver design for 1.2 kv sic module with pcb integrated rogowski coil protection circuit," in *2021 IEEE Energy Conversion Congress and Exposition (ECCE)*. IEEE, 2021, pp. 5723–5728.
- [14] K. Wang, X. Yang, H. Li, L. Wang, and P. Jain, "A high-bandwidth integrated current measurement for detecting switching current of fast gan devices," *IEEE Transactions on Power Electronics*, vol. 33, no. 7, pp. 6199–6210, 2018.